This article has been accepted for publication in a future issue of this journal, but has not been fully edited. Content may change prior to final publication. Citation information: DOI 10.1109/ACCESS.2018.2871244, IEEE Access

IEEE Access
Multidisciplinary | Rapid Review | Open Access Journal

Date of publication xxxx 00, 0000, date of current version xxxx 00, 0000.

Digital Object Identifier 10.1109/ACCESS.2017.Doi Number

A novel position-based impedance control method for bionic legged robots' HDU

Kaixian Ba[1](IEEE member), Bin Yu[1,2]*(IEEE member), Guoliang Ma[1](IEEE student member), Qixin Zhu[1], Zhengjie Gao[1](IEEE student member), and Xiangdong Kong[1,2]

[1]School of Mechanical Engineering, Yanshan University, Qinhuangdao 066004, China

[2]Hebei Provincial Key Laboratory of Heavy Machinery Fluid Power Transmission and Control, Qinhuangdao, China

Corresponding author: Bin Yu (e-mail: yb@ysu.edu.cn, telephone number: +86-335-8074618).

Funding: This study was funded by National Natural Science Foundation of China (Grant No. 51605417), National Key Basic Research Program of China (973 Program, No. 2014CB046405), Doctoral Fund Project of Yanshan University(Grant No. BL18027).

ABSTRACT In this paper, a novel impedance control method is designed for the hydraulic drive unit (HDU) equipped on the hydraulic driven legged robot. Firstly, the position control mathematical model of HDU is built. Next, the HDU performance test platform is introduced and the performance requirements are given. Secondly, the system load pressure observer is designed and an accurate stiffness control method is proposed by combining the external load force feedforward control with the load force feedback control. Thirdly, the damping control method based on the velocity feedback is designed. Finally, a novel impedance control method is proposed through combining the stiffness control and the damping control. The effects of all techniques listed above have been verified experimentally. Especially, the impedance control effects are verified by comparing the impedance characteristics with the natural characteristics of the second-order mass-spring-damper system. The research indicates that the system characteristics of HDU with the novel impedance control method is well equivalent to that of the second-order mass-spring-damper system, which can solve the stall problem of the robot joint movement process caused by the load force vanish instantaneously and the switch between position control and force control. The above research can provide references for the active compliance control of bionic legged robots.

INDEX TERMS Bionic legged robot, Hydraulic drive unit (HDU), Position-based impedance control, Active compliance control, Feedforward compensation control

I. INTRODUCTION

Compared with wheeled robots and crawler robots, legged robots are better at adapting to unknown and unstructured environment especially in the complex wild environment where the robots can execute tasks such as exploration, transportation, rescue and military aid. With the advantages such as small size, high output power, fast response speed and high accuracy, hydraulic drive well fits the high-performance requirements of the legged robots, compared with the motor drive and the pneumatic drive. Therefore, the hydraulic drive is receiving more attention in the legged robots research field[1-4]. Taking the hydraulic drive quadruped robot Big-Dog designed by the Boston Company as an example, the Big-Dog is imitated from the normal quadruped mammal, and has some excellent moving performances such as walk, trot, gallop, bounding 1m width moat and spanning 35° ramp, and can adapt complex landform including mountains, jungles, beaches, swamps, ice and snow with large load mass, which can improve the civilian and military application value of the Big-Dog and make many countries develop the hydraulic driven legged robot research[5-6].

Due to the structure size restrictions and the crawl requirements of the hydraulic motor, the highly integrated valve-controlled cylinder called hydraulic drive unit (HDU) is taken as a driver for the active moving joint of the hydraulic driven legged robots[7-8]. When the legged robots contact the environment in the moving process, the frequent interacting load force exists between the foot end and the ground, so the HDU not only requires fast response and high accuracy but requires compliance to effectively reduce the impact of the hydraulic system, which can protect robot physical construction and installed component from being damaged. With the above issues, many experts developed the active compliance control research. Hogan[9] provided a common active compliance control called impedance control method that didn't need directly control the desired load force and displacement but controlled the dynamic

This work is licensed under a Creative Commons Attribution 3.0 License. For more information, see http://creativecommons.org/licenses/by/3.0/.

This article has been accepted for publication in a future issue of this journal, but has not been fully edited. Content may change prior to final publication. Citation information: DOI 10.1109/ACCESS.2018.2871244, IEEE Access

relationship between the load force and the displacement to achieve the active compliance control. And Maples[10] summed up the impedance control brought up by Hogan[9], deeming that when the load force feedback signal was conversed to displacement error, the stiffness control could be achieved, when the load force feedback signal was conversed to velocity error, the damping control could be achieved and the impedance control could be achieved by combing the stiffness control and the damping control. Generally, this position-based impedance control, which consisted of the impedance control outer loop and the position control inner loop, is the most common method outer loop inner loop, whose schematic is shown in Fig. 1 where the dynamic relationship between the load force and the displacement is built through collecting the load force signal and adjusting the given displacement to simulate the second-order mass-spring-damper system characteristics. In details, the given displacement minus the displacement error generating by the outer loop controller is the desired displacement and the inner loop controller should ensure the actual displacement to track the desired displacement, which can make the robot joints have the compliance that is similar to the second-order mass-spring-damper system[11].

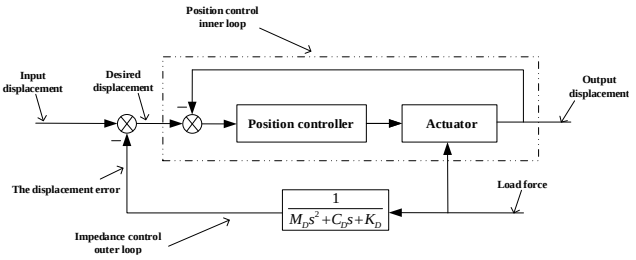

FIGURE 1. The position-based impedance control schematic

Based on the impedance control schematic shown in Fig.1, many experts developed the active compliance control. Heinrichs[12] applied the impedance control to the hydraulic manipulators, making the hydraulic manipulators have some compliance. Bilodeau[13] raised a model-based impedance control scheme for high performance hydraulic joints, and the developed controller is useful in achieving a desired behavior of hydraulic manipulators in contact tasks. Sadjadian[14] applied a model-based impedance control strategy to a 3-DOF parallel manipulator to manage the interaction of the robot with the environment, and it was observed that although the proposed controller was designed for impedance adjustment of the robot, in case of free motion, it resulted into desired position tracking. Minyong[15] applied the hybrid impedance and force control to a multi-fingered robot hand, indicating that this control method was able to create the movement and force of robot to behave as similar as the human's massage. Ioannis[16] applied a novel model-based impedance controller to a 6-DOF electrohydraulic Stewart platform, showing that the impedance controller was superior to available PD controllers, and that its response is smooth. As the hydraulic driven legged robot has received more attention in recent years, the impedance control of the hydraulic legged robots has been especially targeted now. Irawan[17] applied single-leg impedance control and center of mass-based impedance control to the hexapod robot named COMET-IV. These two methods had the same schematic, but the online impedance parameters adjustment accorded to the robot legs' configuration and robot body's configuration respectively, and evaluation and verification experiments were conducted in the laboratory and the actual field with uneven terrain and extremely soft surfaces, indicating that center of mass-based impedance control improved the online impedance parameters adjusting speed and enhancing the impedance control effects. Lee[18] presented position-based impedance control of a hydraulic actuator for a walking robot whose hydraulic actuator was simplified as a linearized model in the impedance control design and hydraulic parameters were verified experimentally, while the effects of the impedance control applied to the hydraulic actuator with the lack of the knowledge of the environmental stiffness were also verified experimentally. Ugurlu[19] presented a trajectory generator and an active compliance control scheme for the HyQ quadruped robot, where the impedance control method was applied to the active compliance controller. Meanwhile, the damping and the stiffness were adjustable online through combining the designed trajectory generator, showing that the active compliance controller was also observed to be efficient in handling environmental interaction while the HyQ robot was trot-walking. Sharifi[20] presented four nonlinear model reference adaptive impedance controllers for human-robot interactions, and compared with the control of the robot impedance with uncertainties in model parameters. The effectiveness of the proposed controllers was investigated by simulations and experiments on a two-DOFs robot. Irawan[21] presented that the self-tuning impedance control was designed with variable stiffness tuning method by using time division method and exponential time reduction, and the proposed controller was verified by walking experiments on several layers of square rubber plate, indicating that the self-tuning impedance control with adaptive element from environment identification could provide compliant body balance for hydraulic-actuated hexapod robot experimentally. Qingsong Xu[22] presented a new robust impedance control for high-speed position and force regulation of a compliant gripper which was driven by a piezoelectric stack actuator , and the effectiveness of the proposed scheme was verified through experimental studies on grasp–hold–release operation of a graphite micro rod, indicating that the proposed scheme enables a smooth transition between the free and constrained motions of the gripper.

However, for the impedance control is based on the dynamic relationship between the load force and the displacement, when the load force on the joints is zero or very small, the displacement error of the impedance control outer loop is very small, whatever the desired damping is, the

This work is licensed under a Creative Commons Attribution 3.0 License. For more information, see http://creativecommons.org/licenses/by/3.0/.

This article has been accepted for publication in a future issue of this journal, but has not been fully edited. Content may change prior to final publication. Citation information: DOI 10.1109/ACCESS.2018.2871244, IEEE Access

effects of damping control are hardly achieved, and the moving velocity of the actuator wouldn't be controlled by the impedance control method. Similarly, not only does the legged robot joint need damping to consume energy under load force, but also the HDU should have some damping characteristics to avoid the stall problem of the robot joint movement process caused by the load force vanish instantaneously and the switch between position control and force control. So it is necessary to research the more applicable impedance control method of the HDU to improve the damping control under zero or small load force. Moreover, the natural hydraulic system stiffness, which has effects on the stiffness control accuracy in the position control process, is all ignored in the above impedance control researches, but for improving the accuracy of the HDU stiffness control, the natural hydraulic system stiffness should be compensated to enhance the HDU stiffness control effects. Taking the above issues into consideration, a novel position-based impedance control method is proposed in this paper, basing on the HDU natural characteristics.

In the authors' former researches, firstly, the system modeling method is proposed to aim at the HDU position control system. Then the position control performance is analyzed. Besides, the sensitivity characteristic, which can evaluate the effect of the system parameters on the position control performance, is researched[23,24]. Secondly, aimed at the HDU force control system, the system modeling method is proposed. And the force control system robust control, under the condition of variable load characteristics, is researched[25]. Those former researches lay the foundation for the mathematical model of position-based impedance control and the inner loop compensation control which are proposed in this paper.

Combined with the analysis mentioned above, the novelty and organization of this paper are listed as follows. Firstly, Position control system block diagram and state space equations of HDU are presented, and the impedance control requirements of HDU are given. Secondly, the stiffness control method of HDU through combing the external load force feedforward control with the load force feedback control is provided. Thirdly, the damping control method of HDU through combing the load pressure observer with the velocity feedback control is provided. Finally, a novel impedance control method is designed through combining the stiffness control with the damping control, and the impedance control experimental curves are compared with the second-order mass-spring-damper system characteristics to verify the effects of the impedance control. The methods listed above improve the damping control of the HDU under no-load or small-load. Compared with the traditional impedance control method, the impedance control method proposed in this paper not only makes the system have the impedance characteristic like traditional impedance control, but can achieve damping control alone. Meanwhile, it can avoid the stall problem of the robot joint movement process caused by the load force vanish instantaneously and switch between position control and force control.

II. Introduction of HDU and Its Test Platform

A. Mathematical model of HDU

As the driver of the leg joint on bionic legged robots, the HDU is a highly integrated system of servo valve-controlled symmetrical cylinder. The author's institute participates in the design of the hydraulic quadruped robot. The quadruped robot prototype, single leg, and HDU performance test platform are shown in Fig. 2 (a)–(c), respectively.

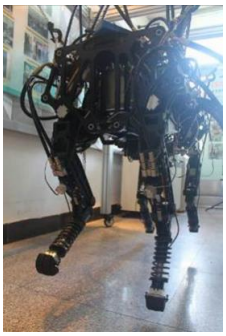

(a) prototype of quadruped robot

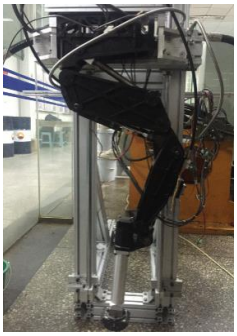

(b) leg hydraulic drive system

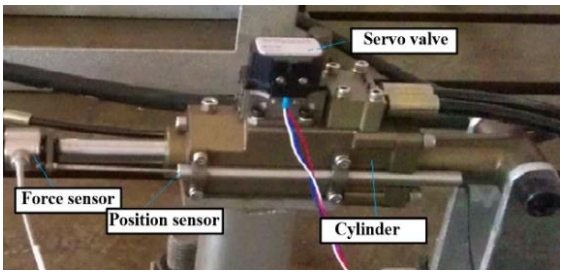

(c) HDU

FIGURE 2. Photos of performance test platform

The closed loop position control block diagram of HDU is shown in Fig. 3.

This work is licensed under a Creative Commons Attribution 3.0 License. For more information, see http://creativecommons.org/licenses/by/3.0/.

This article has been accepted for publication in a future issue of this journal, but has not been fully edited. Content may change prior to final publication. Citation information: DOI 10.1109/ACCESS.2018.2871244, IEEE Access

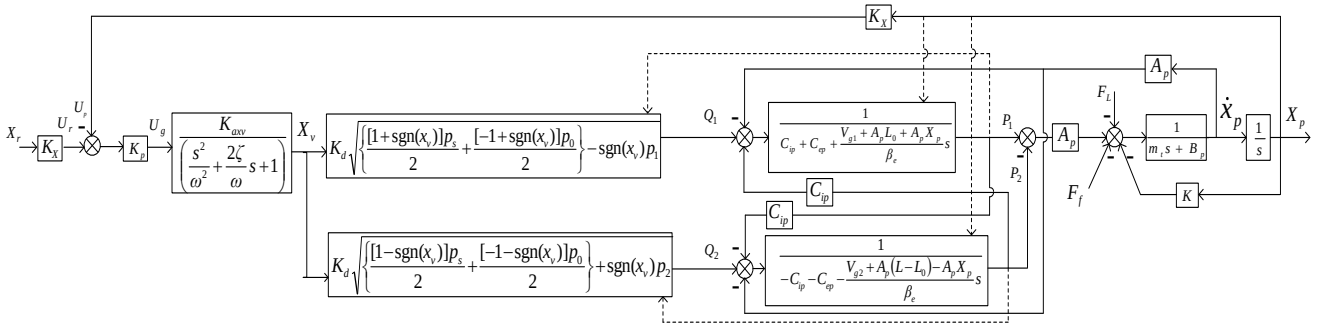

FIGURE 3. Position control system block diagram of HDU

Based on the traditional linear mathematical model of valve-controlled cylinder, the factors containing dynamic characteristics of servo valve, flow-pressure nonlinearity, initial piston position of servo cylinder and friction nonlinearity are considered to ensure the accuracy of mathematical model. And this mathematical model is the foundation of the impedance control in this paper.

B. The performance test platform of HDU

The performance test platform of HDU, whose schematic is shown in Fig. 4. The left channel, which consists of small servo valve, servo cylinder, displacement sensor and force sensor, is the tested HDU. While the right channel is the load simulation part, consisting of the same type servo valve and servo cylinder. The two channels are connected by the force sensor. And the photo of HDU performance test platform is shown in Fig. 5.

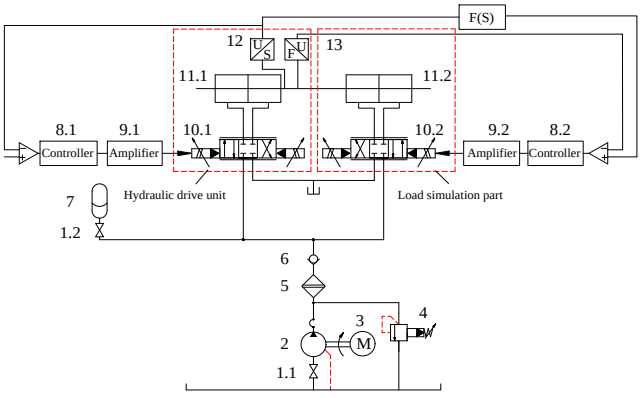

1 globe valve, 2 axial piston pump, 3 electromotor, 4 relief valve, 5 high-pressure filter, 6 check valve, 7 accumulator, 8 dSPACE controller, 9 servo valve amplifier, 10 servo valve, 11 servo cylinder, 12 displacement sensor, 13 force sensor.

FIGURE 4. Schematic of performance test platform of HDU

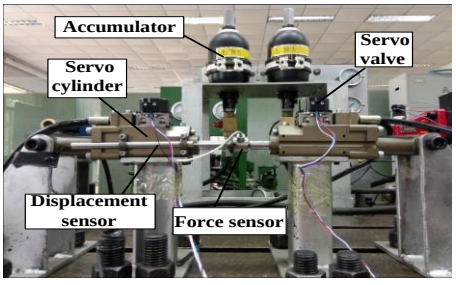

FIGURE 5. Photo of HDU performance test platform

C. Impedance control requirements of HDU

The characteristics which are similar to second-order mass-spring-damper system shown in Fig. 6 should exist in HDU to ensure active compliance of the hydraulic drive legged robots. Yet HDU and second-order mass-spring-damper system are different, the difference is that the second-order mass-spring-damper system is passive system, because the force on system is the driving force which makes the mass move passively. But HDU is the active system, because the force on M_D is load force rather than driving force .

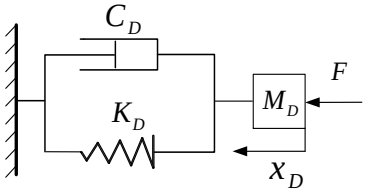

FIGURE 6. Schematic of second-order mass-spring-damper system

Due to the piston reciprocating motion in the oil, HDU has the damping characteristics, and the natural stiffness exists in the position control system of HDU. Yet damping of HDU is quite small, and the stiffness of HDU is large and not constant, compared with the desired stiffness K_D and the desired damping C_D in impedance control of legged robot joints. Moreover, the mechanical structures having the characteristics of second-order mass-spring-damper system that don't exist in HDU, so that virtual spring and damper whose schematic is shown in Fig.7 should be constructed inside HDU to ensure the desired impedance characteristics of HDU.

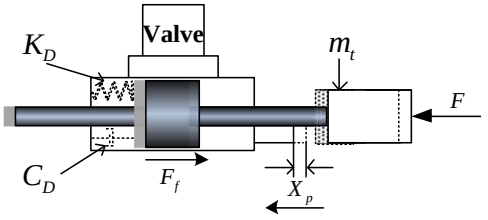

FIGURE 7. Virtual impedance schematic of HDU

This work is licensed under a Creative Commons Attribution 3.0 License. For more information, see http://creativecommons.org/licenses/by/3.0/.

This article has been accepted for publication in a future issue of this journal, but has not been fully edited. Content may change prior to final publication. Citation information: DOI 10.1109/ACCESS.2018.2871244, IEEE Access

In order to obtain the impendence characteristics shown in Fig. 7, an equation can be constructed as follows:

$$p_L A_p = m_t \ddot{x}_p + C_D \dot{x}_p + K_D x_p + F + F_f . \quad (1)$$

If Eq. (1) is constantly valid in the control progress, which can be equivalent to exist a spring having desired stiffness K_D and a damper having desired damping C_D, the characteristics of impendence control will be obtained. In the following sections, the desired stiffness is contained in the accurate simulation, and will be researched respectively to obtain impendence control method of HDU based on Eq. (1), so does the desired damping.

III. Stiffness Control Method of HDU

A. The principle of stiffness control

The position control accuracy is affected by the load force disturbance in the position loop control process, K_s refers to the closed loop system stiffness of HDU. So, the stiffness control is that K_s and K_D in series and the schematic is shown in Fig. 8.

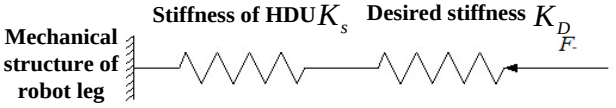

FIGURE 8. Equivalent spring series schematic

As it can be seen in Fig. 8, and the synthetical stiffness of system can be expressed as follows

$$K_s' = \frac{1}{\frac{1}{K_s} + \frac{1}{K_D}} . \quad (2)$$

It can be seen in Eq.(2), if the closed loop system stiffness K_s is much bigger than the desired stiffness K_D, the synthetical stiffness K_s' will approach to the desired stiffness K_D, which will improve the stiffness control accuracy. Therefore, the method which can enhance the closed loop system stiffness K_s should be researched firstly, and then the simulation of the desired stiffness K_D can be researched.

B. Method of enhancing the closed loop system stiffness

The effects of the load force on the position control accuracy can be reduced significantly by enhancing the closed loop system stiffness K_s. Therefore, the corresponding compensation control method need to be adopted to reduce the effects of load force on the position control system output.

The force equilibrium equation of HDU can be expressed as follows:

$$\ddot{x}_p = \frac{1}{m_t}(p_L A_p - B_p \dot{x}_p - K x_p - F_f - F_L) . \quad (3)$$

The force equilibrium block diagram of HDU is derived and shown in Fig. 9.

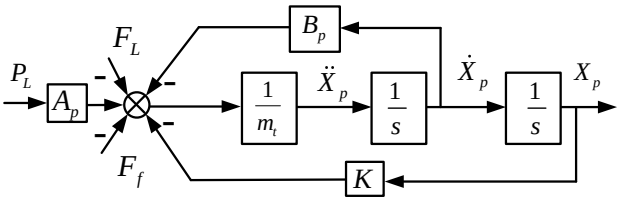

FIGURE 9. Force equilibrium block diagram of HDU

The force equilibrium state space equations of HDU can be expressed as follows:

$$\begin{bmatrix} \dot{p}_L \\ \dot{x}_p \\ \ddot{x}_p \end{bmatrix} = \begin{bmatrix} 0 & 0 & 0 \\ 0 & 0 & 1 \\ \frac{A_p}{m_t} & \frac{-K}{m_t} & \frac{-B_p}{m_t} \end{bmatrix} \begin{bmatrix} p_L \\ x_p \\ \dot{x}_p \end{bmatrix} + \begin{bmatrix} 0 \\ 0 \\ \frac{-1}{m_t} \end{bmatrix} (F_f + F_L) . \quad (4)$$

Based on Eq. (3), $x_1 = x_p$, $x_2 = \dot{x}_p$, $p_L = x_5 - x_6 = p_1 - p_2$ and denote the summation of F_f and F_L as u, that is $u = F_f + F_L$. And the derivative of load pressure $\dot{p}_L = 0$ under the steady state condition, so the Eq. (4) can be expressed as follows:

$$\begin{bmatrix} \dot{p}_L \\ \dot{x}_1 \\ \dot{x}_2 \end{bmatrix} = \begin{bmatrix} 0 & 0 & 0 \\ 0 & 0 & 1 \\ \frac{A_p}{m_t} & \frac{-K}{m_t} & \frac{-B_p}{m_t} \end{bmatrix} \begin{bmatrix} p_L \\ x_1 \\ x_2 \end{bmatrix} + \begin{bmatrix} 0 \\ 0 \\ \frac{-1}{m_t} \end{bmatrix} u . \quad (5)$$

Denote the output equations as $\boldsymbol{y} = \boldsymbol{C'x}$, the augmented system state space equations of Eq. (3) can be expressed as follows:

$$\begin{cases} \dot{\boldsymbol{X}} = \boldsymbol{A'X} + \boldsymbol{B'u} \\ \boldsymbol{y} = \boldsymbol{C'X} \end{cases} . \quad (6)$$

Denote $\boldsymbol{x_0} = \begin{bmatrix} x_1 & x_2 \end{bmatrix}^T = \begin{bmatrix} x_p & \dot{x}_p \end{bmatrix}^T$, then the Eq.(7) can be expressed as follows:

$$\begin{cases} \begin{bmatrix} \dot{p}_L \\ \dot{\boldsymbol{x}}_0 \end{bmatrix} = \begin{bmatrix} \boldsymbol{A_{11}} & \boldsymbol{A_{12}} \\ \boldsymbol{A_{21}} & \boldsymbol{A_{22}} \end{bmatrix} \begin{bmatrix} p_L \\ \boldsymbol{x_0} \end{bmatrix} + \begin{bmatrix} \boldsymbol{B_0} \\ \boldsymbol{B_1} \end{bmatrix} \boldsymbol{u} \\ \boldsymbol{y} = \begin{bmatrix} 0 & \boldsymbol{C_1} \end{bmatrix} \begin{bmatrix} p_L \\ \boldsymbol{x_0} \end{bmatrix} = \boldsymbol{C x_0} \end{cases} , \quad (7)$$

where, $\boldsymbol{A_{11}} = \boldsymbol{B_0} = 0$, $\boldsymbol{A}_{12} = \begin{bmatrix} 0 & 0 \end{bmatrix}$, $\boldsymbol{A}_{21} = \begin{bmatrix} 0 & \frac{A_p}{m_t} \end{bmatrix}^T$,

$\boldsymbol{A}_{22} = \begin{bmatrix} 0 & 1 \\ \frac{-K}{m_t} & \frac{-B_p}{m_t} \end{bmatrix}$, $\boldsymbol{B}_1 = \begin{bmatrix} 0 & \frac{-1}{m_t} \end{bmatrix}^T$, $\boldsymbol{C}_1 = \begin{bmatrix} 1 & 1 \end{bmatrix}$,

$\boldsymbol{C} = \begin{bmatrix} 0 & 1 & 1 \end{bmatrix}$. $\boldsymbol{x_0}$ and $\dot{\boldsymbol{x}}_0$ are the displacement and the velocity output of HDU respectively which can be measured directly. p_L is the two carves pressure difference of HDU which need to be observed. So, the coefficient matrix rank of Eq. (8) can be expressed as follows:

This work is licensed under a Creative Commons Attribution 3.0 License. For more information, see http://creativecommons.org/licenses/by/3.0/.

This article has been accepted for publication in a future issue of this journal, but has not been fully edited. Content may change prior to final publication. Citation information: DOI 10.1109/ACCESS.2018.2871244, IEEE Access

$$Rank\left[\boldsymbol{C}\quad\boldsymbol{CA}\quad\boldsymbol{CA}^2\right]^T = Rank\begin{bmatrix} 0 & 1 & 1 \\ \frac{A_p}{m_t} & \frac{-K}{m_t} & 1-\frac{B_p}{m_t} \\ \frac{A_p}{m_t}-\frac{A_pB_p}{m_t^2} & \frac{KB_p}{m_t^2}-\frac{K}{m_t} & \frac{B_p^2}{m_t^2}-\frac{B_p}{m_t}-\frac{K}{m_t} \end{bmatrix}, \quad (8)$$

where, $m_t - B_p + K \neq 0$, which can prove that the column and row vector group of the matrix $\left[C\ CA\ CA^2\right]^T$ is linearly independent, so $Rank\left[\boldsymbol{C}\quad\boldsymbol{CA}\quad\boldsymbol{CA}^2\right]^T = 3$. Basing on the observability criterion of the linear time-invariant system, the system state is completely observable.

To get the observable p_L, Eq. (8) can be transformed as follows:

$$\begin{cases} \dot{p}_L = \boldsymbol{A}_{11}p_L + \boldsymbol{A}_{12}\boldsymbol{x}_0 + \boldsymbol{B}_0 u \\ \dot{\boldsymbol{x}}_0 = \dot{\boldsymbol{y}} = \boldsymbol{A}_{21}p_L + \boldsymbol{A}_{22}\boldsymbol{x}_0 + \boldsymbol{B}_1 u \end{cases}. \quad (9)$$

Denote $\boldsymbol{y}_1 = \dot{\boldsymbol{y}} - \boldsymbol{A}_{22}\boldsymbol{y} - \boldsymbol{B}_1\boldsymbol{u}$, so Eq. (9) can be expressed as follows:

$$\begin{cases} \dot{p}_L = \boldsymbol{A}_{11}p_L + (\boldsymbol{A}_{12}y + \boldsymbol{B}_0 u) \\ y_1 = \boldsymbol{A}_{21}p_L \end{cases}. \quad (10)$$

The state variable of Eq. (10) is p_L, the system input is $\boldsymbol{A}_{12}y + \boldsymbol{B}_0 u$ and the system output equation is $y_1 = \boldsymbol{A}_{21}p_L$, so the observer equation can be constructed as follows:

$$\dot{\hat{p}}_L = (\boldsymbol{A}_{11} - \boldsymbol{G}\boldsymbol{A}_{21})\dot{\hat{p}}_L + (\boldsymbol{A}_{12}y + \boldsymbol{B}_0 u) + \boldsymbol{G}y_1, \quad (11)$$

where, $\boldsymbol{G} = [g_1 \quad g_2]$, which is 1×2 order check matrix of the observer, and introduce transformation as follows:

$$\begin{cases} \boldsymbol{w} = \hat{p}_L - \boldsymbol{G}y \\ \dot{\boldsymbol{w}} = \dot{\hat{p}}_L - \boldsymbol{G}\dot{y} \end{cases}. \quad (12)$$

Denote the corresponding order-reduced observer as follows:

$$\begin{cases} \dot{\boldsymbol{w}} = (\boldsymbol{A}_{11} - \boldsymbol{G}\boldsymbol{A}_{21})\boldsymbol{w} + (\boldsymbol{B}_0 - \boldsymbol{G}\boldsymbol{B}_1)u + [(\boldsymbol{A}_{12} - \boldsymbol{G}\boldsymbol{A}_{22}) + (\boldsymbol{A}_{11} - \boldsymbol{G}\boldsymbol{A}_{21})\boldsymbol{G}]y \\ \hat{p}_L = \boldsymbol{w} + \boldsymbol{G}y \end{cases}. \quad (13)$$

To ensure $\hat{p}_L$ approaching to p_L soon, $\boldsymbol{A}_{11} - \boldsymbol{G}\boldsymbol{A}_{21}$ should satisfy the Hurwitz stability criterion so that g_2 is any value greater than 0. In order to facilitate the calculation, g_1 is selected 0.

And, $\boldsymbol{G}$, $\boldsymbol{A}_{11}$, $\boldsymbol{A}_{12}$, $\boldsymbol{A}_{21}$, $\boldsymbol{A}_{22}$, $\boldsymbol{B}_0$ and $\boldsymbol{B}_1$ are taken into Eq.(13), the simplification can be expressed as follows:

$$\dot{\boldsymbol{w}} = \frac{-A_p}{m_t}g_2\boldsymbol{w} + \frac{F_L + F_f}{m_t}g_2 + \frac{K}{m_t}g_2 x_p + \frac{B_p}{m_t}g_2\dot{x}_p - \frac{A_p}{m_t}g_2^2\dot{x}_p. \quad (14)$$

Denote both sides of Eq. (14) is conducted by Laplace transformation as follows:

$$s\boldsymbol{w}(s) = -\frac{A_p}{m_t}g_2\boldsymbol{w}(s) + \frac{F_L(s) + F_f(s)}{m_t}g_2 + \frac{K}{m_t}g_2 X_p(s) + \frac{B_p}{m_t}g_2 sX_p(s) - \frac{A_p}{m_t}g_2^2 sX_p(s). \quad (15)$$

The simplification of Eq. (15) can be expressed as follows:

$$\boldsymbol{w}(s) = \frac{[F_L(s) + F_f(s) + KX_p(s)]g_2 + [B_p - g_2A_p]g_2 sX_p(s)}{m_t s + A_p g_2}. \quad (16)$$

So, the load pressure observer can be expressed as follows:

$$\hat{p}_L = \frac{g_2[F_L(s) + F_f(s) + KX_p(s)] + g_2(B_p + m_t s)sX_p(s)}{m_t s + A_p g_2}. \quad (17)$$

In order to verify the validity of the load pressure observer, it is necessary to keep the position signal of the HDU constant, and use the force signal data tested by force sensor under sine load with a frequency of 5 Hz and amplitudes of 500N and 1000N respectively to observe the load pressure $\hat{p}_L$ by load pressure observer model. The pressure carves of load observation is shown in Fig. 10.

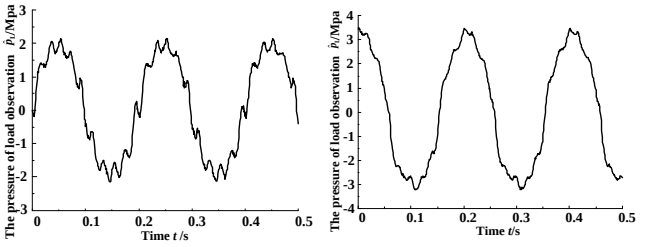

a) 500 N Sine load force **b) 1000 N Sine load force**

FIGURE 10. Pressure carves of load observation

It can be seen in Fig. 10 that the load pressure of the HDU can be observed during using the load pressure observation method, and the observation curve is smoother.

Taking the friction characteristics and external load force as the disturbance to compensate, the position control block diagram of HDU with feedforward link is shown in Fig. 11.

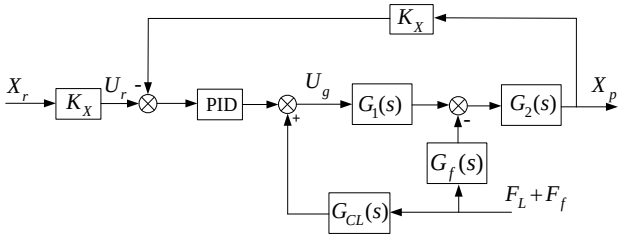

FIGURE 11. Position control block diagram with feedforward link

In Fig. 11, $G_f(s)$ is the disturbance transfer function, $G_1(s)$ and $G_2(s)$ are the transfer functions of different system composition respectively, and $G_{CL}(s)$ is the transfer function of the external load force feedforward compensation controller. So $G_{CL}(s)$ is:

$$G_{CL}(s) = \frac{G_f(s)}{G_1(s)}. \quad (18)$$

Ignoring the effects of the initial displacement of HDU can simplify the control compensation link, so $V_{g1} + A_pL_0 + A_pX_p = V_{g2} + A_p(L - L_0) - A_pX_p = V_t/2$. And based

This work is licensed under a Creative Commons Attribution 3.0 License. For more information, see http://creativecommons.org/licenses/by/3.0/.

This article has been accepted for publication in a future issue of this journal, but has not been fully edited. Content may change prior to final publication. Citation information: DOI 10.1109/ACCESS.2018.2871244, IEEE Access

on the Fig. 1 and Eq. (18), the feedforward compensation controller can be expressed as follows

$$G_{CL}(s)=\frac{\frac{s^2}{\omega^2}+\frac{2\zeta}{\omega}s+1}{K_{qxv}A_p}\left[\frac{C_{ip}+\frac{V_t}{4\beta_e}s}{K_d\sqrt{p_s-p_0-\hat{p}_L}}+\frac{x_v}{2(p_s-p_0-\hat{p}_L)}\right]. \quad (19)$$

where, $\hat{p}_L$ can be obtained from the load pressure observer.

For the second-order differential link is difficult achieving in the actual control process and the natural frequency of the servo valve is much higher than the working frequency of HDU, the second-order differential link is ignored in the compensation link. Basing on Fig. 10, the following equation is:

$$[(X_r-X_p)K_XK_p+(F_L+F_f)G_{CL}(s)]G_1(s)-(F_L+F_f)G_f(s)=\frac{X_p}{G_2(s)}. \quad (20)$$

The stiffness of position control system of HDU represents the disturbance rejection ability, and the bigger the stiffness is, the higher the disturbance rejection ability is. Only should the transfer function relationship between external load force and output displacement be established to research the system stiffness, so deem $X_r=0$, define:

$$K_1=\begin{cases}K_d\sqrt{p_s-p_1} & x_v\geq 0\\ K_d\sqrt{p_1-p_0} & x_v<0\end{cases}, \quad (21)$$

$$K_2=\begin{cases}K_d\sqrt{p_2-p_0} & x_v\geq 0\\ K_d\sqrt{p_s-p_2} & x_v<0\end{cases}. \quad (22)$$

Ignoring the second-order oscillation link, and the closed loop system stiffness with the feedforward compensation can be expressed as follows:

$$\frac{F_L+F_f}{X_p}=\frac{\frac{m_tV_t^2}{4\beta_e^2}s^3+\frac{4\beta_em_tC_{ip}V_t+B_pV_t^2}{4\beta_e^2}s^2+\left[\frac{KV_t^2}{4\beta_e^2}+\frac{(B_pC_{ip}+A_p^2)V_t}{\beta_e}\right]s+\frac{KC_{ip}V_t}{\beta_e}}{(\frac{K_1+K_2}{\hat{K}_2+\hat{K}_1}-1)\frac{V_t^2}{4\beta_e^2}s+(\frac{K_1+K_2}{\hat{K}_2+\hat{K}_1}-1)\frac{V_tC_{ip}}{\beta_e}}. \quad (23)$$

As it can be seen in Eq. (23), when $\hat{p}_L\to p_L$, the two calculated cavity pressure $\hat{p}_1\to p_1$, $\hat{p}_2\to p_2$, $\hat{K}_1\to K_1$ and $\hat{K}_2\to K_2$, and the system stiffness $(F_L+F_f)/X_p\to\infty$, so the closed loop system stiffness K_s is infinite in theory. And the feedforward compensation control schematic is shown in Fig. 12.

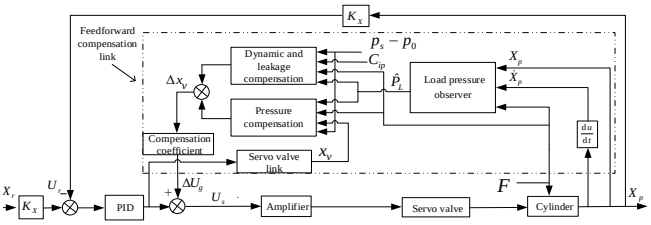

FIGURE 12. Feedforward compensation control schematic

C. Schematic of stiffness control

A feedforward compensation control is introduced to ensure that the closed loop system stiffness is much bigger than the desired stiffness, then the desired displacement error caused by the load force is transformed to voltage signal to make HDU simulate a spring which has the desired stiffness, and the stiffness control schematic of HDU is shown in Fig. 13.

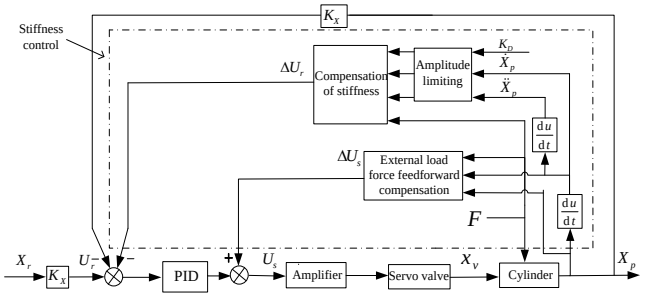

FIGURE 13. Stiffness control schematic of HDU

D. Experiment of stiffness control

In order to clearly analyze whether the HDU position control system under the stiffness control is linear, this section presents the HDU displacement response experiments under 1000 N ramp loading with target stiffnesses of $K_D=1\times10^6$ N/m and $K_D=2\times10^6$ N/m respectively. The measured curves of the loading force are given in Fig. 14.

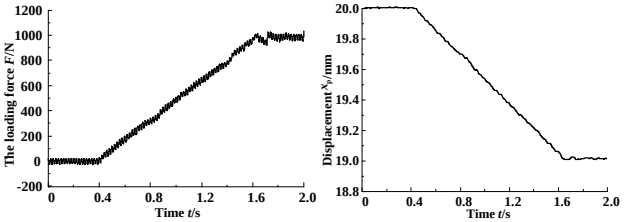

(a) load force curve with $K_D=1\times10^6$ N/m **(b) Stiffness control response curve**

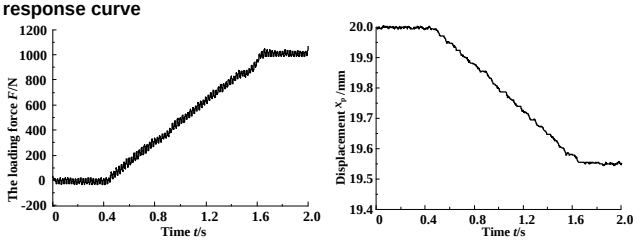

(c) load force cure with $K_D=2\times10^6$ N/m **(d) Stiffness control response curve**

FIGURE 14. Stiffness control curves

According to the Fig. 14, the displacement of the HDU changes linearly with the change of the load force. It is known from Hooke's Law that the stiffness of the system is a constant value, when the load force reaches 1000 N, the corresponding displacement errors are 10 mm and 5 mm respectively, which proves that the stiffness control is effective.

Ⅳ. Damping control method of HDU

This work is licensed under a Creative Commons Attribution 3.0 License. For more information, see http://creativecommons.org/licenses/by/3.0/.

This article has been accepted for publication in a future issue of this journal, but has not been fully edited. Content may change prior to final publication. Citation information: DOI 10.1109/ACCESS.2018.2871244, IEEE Access

A. Mathematical model of damping control

According to impedance control requirements of HDU shown in section II. C, the simulated damper whose damping value is C_D inside HDU should be constructed to achieve the damping control of HDU, and denote the relationship between the damping force and the velocity as follows:

$$F_c = C_D \dot{x}_p . \tag{24}$$

The direction of the damping force F_c is opposite to the velocity direction of HDU, and denote the load pressure of HDU as follows:

$$p_L = \frac{m_t \ddot{x}_p + F + F_f + F_c}{A_p} . \tag{25}$$

Basing on the servo valve flow equation and the flow continuity equation, denote the output flow of the servo valve as follows:

$$\begin{cases} q = K_d x_v \sqrt{p_s - p_0 - p_L} \\ q = A_p \dot{x}_p + C_{ip} p_L + \dfrac{V_1}{4\beta_e} \dot{p}_L \end{cases} . \tag{26}$$

When the damping control is not adopted, the load pressure of HDU can be expressed as follows:

$$p_L' = \frac{m_t \ddot{x}_p' + F' + F_f}{A_p} . \tag{27}$$

Basing on the servo valve flow equation and the flow continuity equation, denote the output flow of the servo valve as follows:

$$\begin{cases} q' = K_d x_v' \sqrt{p_s - p_0 - p_L'} \\ q' = A_p \dot{x}_p' + C_{ip} p_L' + \dfrac{V_1}{4\beta_e} \dot{p}_L' \end{cases} . \tag{28}$$

Load pressure variation of the HDU caused by the simulated damper, which is feedback damping pressure, can be expressed as follows:

$$p_c = p_L - p_L' . \tag{29}$$

As it can be seen, if the damper exists, the increase of the load pressure of the HDU leads the output flow of the servo valve decreasing, which restrains moving velocity of the HDU. Yet the above damper doesn't exist in the actual position control of the HDU and the load pressure is determined by the load characteristics.

Basing on the Eq. (29), denote the spool displacement with damp control as follows:

$$x_v = \frac{A_p \dot{x}_p + C_{ip} p_L + \dfrac{V_t}{4\beta_e} \dot{p}_L}{K_d \sqrt{p_s - p_0 - p_L}} . \tag{30}$$

Basing on the Eq. (30), denote the spool displacement without damping control as follows:

$$x_v' = \frac{A_p \dot{x}_p' + C_{ip} p_L' + \dfrac{V_t}{4\beta_e} \dot{p}_L'}{K_d \sqrt{p_s - p_0 - p_L'}} . \tag{31}$$

Denote the spool displacement compensation value under the damping control as follows:

$$\Delta x_v = x_v' - x_v . \tag{32}$$

And the corresponding input voltage signal can be expressed as follows:

$$\Delta U_s = \frac{\Delta x_v}{K_{axv}} . \tag{33}$$

Combining equations from Eq. (30) to Eq. (33), the following is:

$$\Delta U_s = \left(\frac{A_p \dot{x}_p' + C_{ip} p_L' + \dfrac{V_t}{4\beta_e} \dot{p}_L'}{K_d \sqrt{p_s - p_0 - p_L'}} - \frac{A_p \dot{x}_p + C_{ip} p_L + \dfrac{V_t}{4\beta_e} \dot{p}_L}{K_d \sqrt{p_s - p_0 - p_L}} \right) / K_{axv} . \tag{34}$$

Therefore, the Eq. (34) can be fulfilled through controlling the voltage to achieve the damping control of HDU.

B. Schematic of damping control

The main idea of damping control is organized as follows: the equivalent voltage variation ΔU_s is caused by feedback damping force F_c which is the product of the piston velocity tested online and the desired damping, and it makes the HDU achieve damping control, according to the basic equations of hydraulic system and the load pressure observer shown in section III. B And the damping control block diagram of the HDU is shown in Fig. 15.

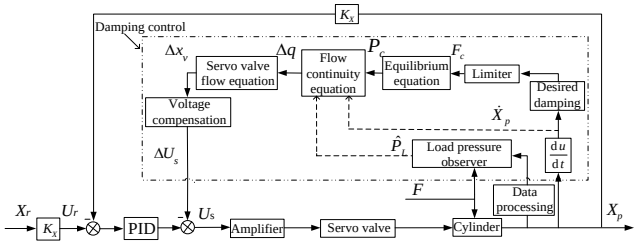

FIGURE 15. Damping control schematic diagram of HDU

C. Experiment of no load damping control effect

In order to prove the feasibility of the damping control of the HDU, the damping control experiment under the no-load and constant load force are given respectively. The specific experiments are shown as follows.

The desired damping (C_D) is set to 0Ns/m, 5×10^4 Ns/m and 1×10^5 Ns/m respectively. Through the experimental test, equivalent damping control effect curves, which is shown in the Fig.16, can be obtained under the HDU under no-load conditions.

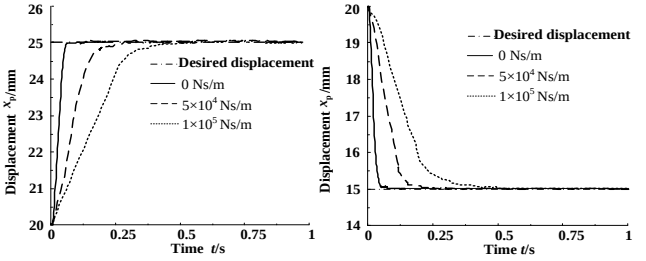

(a) +5 mm step **(b) -5 mm step**

FIGURE 16. Damping control curves without load

This work is licensed under a Creative Commons Attribution 3.0 License. For more information, see http://creativecommons.org/licenses/by/3.0/.

This article has been accepted for publication in a future issue of this journal, but has not been fully edited. Content may change prior to final publication. Citation information: DOI 10.1109/ACCESS.2018.2871244, IEEE Access

It can be seen from the Fig. 16 that there are damping effects in the step response of no-load. Under the three desired damping parameters, the rise time is extended from the initial 40ms to 240ms and 450ms, respectively, which proves the effectiveness of the damping control.

D. Experiment of damping control under constant force loading

To verify the damping control effect of the HDU subjected to press/pull bidirectional loading force, the input displacement step is 5mm. The experimental effect curve of the control effect is shown in the Fig. 17.

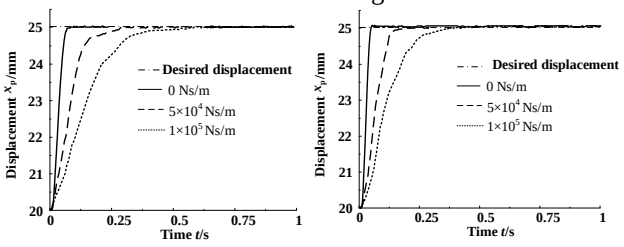

(a) +5 mm step under 500 N press **(b) -5 mm step under 500 N pull**

FIGURE 17. Damping control curves with bi-directional load force

As it can be seen from the Fig. 17 that the step response of the HDU has a damping effect under press and pull load conditions, and the damping control method in this section can effectively limit the movement speed of the HDU, avoiding the stall problem of the robot joint movement process caused by the load force vanish instantaneously and the switch between position control and force control.

Ⅴ. Impedance control method of HDU

A. Schematic of impedance control

The stiffness control and damping control are achieved in above sections, the schematic of impedance control shown in Fig. 18 can be obtained by Fig. 13 and Fig. 15.

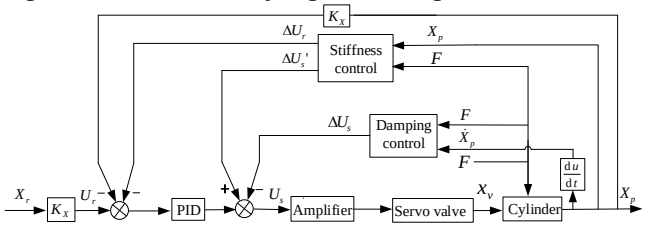

FIGURE 18. Impedance control schematic of HDU

B. Experiment of impedance control under typical load force

Two groups of impedance parameters which are $C_D = 5\times10^4$ Ns/m, $K_D = 1\times10^6$ N/m and $C_D = 1\times10^5$ Ns/m, $K_D = 2\times10^6$ N/m are selected. The load force curves and the displacement output experimental curves with the above two groups of impedance parameters under typical load force are shown in Fig. 19, and the comparison between the stiffness control and the impedance control is also shown in Fig. 19 to present the impedance control effects.

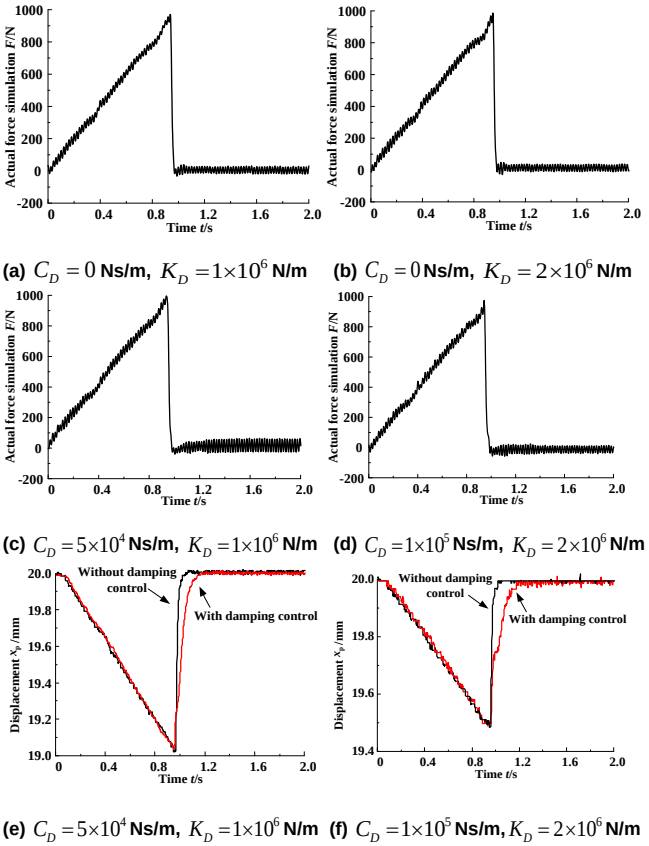

(a) $C_D = 0$ **Ns/m,** $K_D = 1\times10^6$ **N/m** **(b)** $C_D = 0$ **Ns/m,** $K_D = 2\times10^6$ **N/m**

(c) $C_D = 5\times10^4$ **Ns/m,** $K_D = 1\times10^6$ **N/m** **(d)** $C_D = 1\times10^5$ **Ns/m,** $K_D = 2\times10^6$ **N/m**

(e) $C_D = 5\times10^4$ **Ns/m,** $K_D = 1\times10^6$ **N/m** **(f)** $C_D = 1\times10^5$ **Ns/m,** $K_D = 2\times10^6$ **N/m**

FIGURE 19. Experiment curves of ramp load force and displacement response

The impedance control effects of the first group of the impedance parameters are taken as an example shown in Fig. 19-e, when the load force vanishes instantaneously at 1s, the displacement output of HDU move to 20 mm slowly under impedance control relative to only stiffness control, which present the impedance control effect can avoid the stall problem caused by the load force vanish instantaneously. Furthermore, about 20ms response time is needed to obtain the damping control effect, which is the natural deficiency of the existing active compliance control method, and the length of this response time is determined by the natural characteristic of the HDU position control system.

C. Experiment of impedance control under sine load force

The load force curves and the displacement output experimental curves with the above two groups of impedance parameters under sine load force corresponding to frequency 2Hz and amplitude 1000N are shown in Fig. 20.

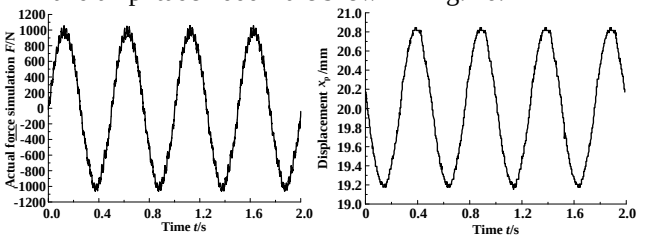

This work is licensed under a Creative Commons Attribution 3.0 License. For more information, see http://creativecommons.org/licenses/by/3.0/.

This article has been accepted for publication in a future issue of this journal, but has not been fully edited. Content may change prior to final publication. Citation information: DOI 10.1109/ACCESS.2018.2871244, IEEE Access

(a) $C_D = 5\times10^4$ **Ns/m,** $K_D = 1\times10^6$ **N/m** **(b)** $C_D = 5\times10^4$ **Ns/m,** $K_D = 1\times10^6$ **N/m**

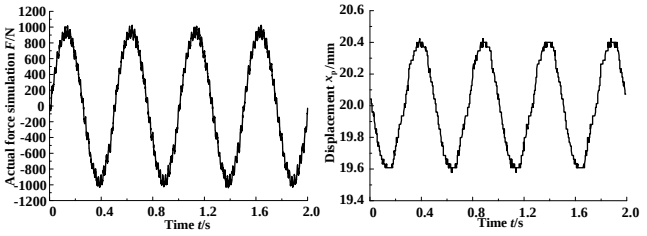

(c) $C_D = 1\times10^5$ **Ns/m,** $K_D = 2\times10^6$ **N/m** **(d)** $C_D = 1\times10^5$ **Ns/m,** $K_D = 2\times10^6$ **N/m**

FIGURE 20. Experiment curves of sine load force and displacement output of impedance control

As it can be seen in Fig. 20, the displacement output has sinusoidal variation with the corresponding load force sinusoidally varying so that the impedance control effects have been achieved. The theoretical amplitudes of the displacement output are 1mm and 0.5mm respectively with the above two groups of impedance parameters, yet the actual amplitudes of the displacement output which are about 0.8mm and 0.4mm respectively cannot reach the theoretical one due to the damping control.

D. Experiment of impedance control under sine load force

In order to test the robustness of the control method. The impedance control experiments were given. The specific experiments are shown as follows.

The two sets of impedance characteristic parameter were mentioned ($C_D = 5\times10^4$ Ns/m, $K_D = 1\times10^6$ N/m and $C_D = 1\times10^5$ Ns/m, $K_D = 2\times10^6$ N/m), the random load force is given(the following figure-a), the impedance control response curve (the following Fig. 21(b)), the Impedance control error curve(the following Fig. 21(c)) are shown in Fig. 21 and Fig. 22.

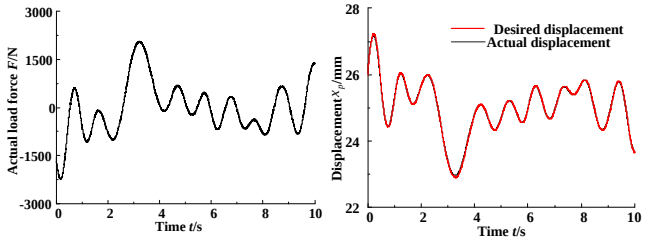

(a) Random load force curve **(b) Impedance control response curve**

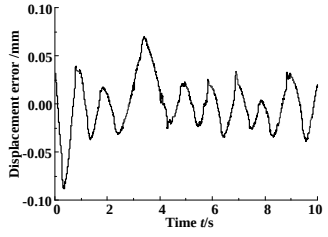

(c) Impedance control error curve

FIGURE 21. Impedance control experimental curves under the random force with $C_D = 5\times10^4$ **Ns/m,** $K_D = 1\times10^6$ **N/m**

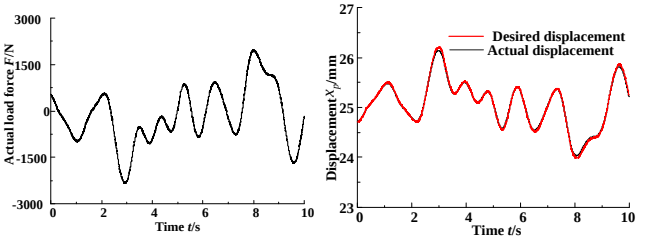

(a) Random load force curve **(b) Impedance control response curve**

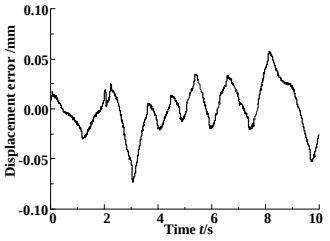

(c) Impedance control error curve

FIGURE 22. Impedance control experiment under the random force with $C_D = 1\times10^5$ **Ns/m,** $K_D = 2\times10^6$ **N/m**

As it can be seen from Fig. 21 and Fig. 22 that under the random load force, HDU can achieve impedance characteristics. It can be seen from the figure-(c) (impedance control error curve) in Fig. 21 and Fig. 22 that the range of error variation within 0.1mm under the random load force, indicating that the proposed impedance control method has well adaptability.

D. Verification of impedance control effects

In this paper, the position control system of the HDU should be approximately equivalent to the second-order mass-spring-damper system, which is the purpose of the impedance control. If the experiment curves of impedance control approximately coincide with those of second-order mass-spring-damper system, the accuracy of impedance control would be verified.

The kinetic model of second-order mass-spring-damper system is shown in Fig. 23.

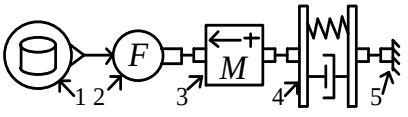

1 function of load force, 2 module convert a dimensionless signal input to a force with the same value, 3 mass module, 4 stiffness and damping modules, 5 zero velocity source

FIGURE 23. Dynamic model of second-order mass-spring-damper system

The stiffness and damping parameters of this kinetic model are same to those of the above research, the load force experimental curves shown in Fig. 20 and 21 are taken as the input of the kinetic model in order to ensure the same input

This work is licensed under a Creative Commons Attribution 3.0 License. For more information, see http://creativecommons.org/licenses/by/3.0/.

This article has been accepted for publication in a future issue of this journal, but has not been fully edited. Content may change prior to final publication. Citation information: DOI 10.1109/ACCESS.2018.2871244, IEEE Access

of the kinetic model and impedance control, then the displacement output curves of second-order mass-spring-damper system are shown in Fig. 24 under typical load force and sine load force.

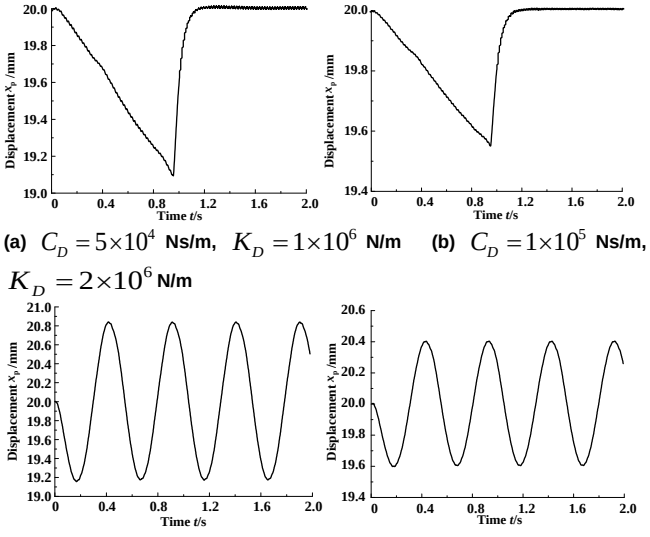

(a) $C_D = 5\times10^4$ Ns/m, $K_D = 1\times10^6$ N/m (b) $C_D = 1\times10^5$ Ns/m, $K_D = 2\times10^6$ N/m

(c) $C_D = 5\times10^4$ Ns/m, $K_D = 1\times10^6$ N/m (d) $C_D = 1\times10^5$ Ns/m, $K_D = 2\times10^6$ N/m

Fig. 24. The displacement output curves of second-order mass-spring-damper system

The displacement output curves comparison between the second-order mass-spring-damper system and the impedance control of the HDU under two kinds of load force, which can be seen in Fig. 20, 21 and 26, indicates the same tendency and the similar value. Taking the sine load force as an example, the amplitudes of the second-order mass-spring-damper system with two groups of impedance parameters are 0.8mm and 0.4mm respectively, which are same to the experiment results shown in section V. B, so that the impedance control effects can be verified.

VI. Conclusion

This paper proposes a novel position-based impedance control method for the HDU. The feasibility and the effects of the impedance control are verified through the experiments of the stiffness control, the damping control and the impedance control respectively. The conclusions are shown as follows:

Firstly, the stiffness control method is proposed by combing the external load force feedforward and the load force feedback to achieve the online displacement change of the HDU under different load force, indicating that the HDU stiffness control has high accuracy.

Secondly, the damping control method is proposed by combing the velocity feedback and the load pressure observer to make the HDU have damping effects whether there is load forces applied to the system. So, the velocity of HDU can be limited effectively and the stall problem of the HDU can be settled. By contrast, the traditional position-based damping control method can hardly make the HDU have damping characteristics under small load or no load.

Finally, a novel impedance control method is proposed by combing the stiffness control and the damping control to obtain the impedance characteristics of the HDU. The experimental effects approximately coincide with the response characteristics of the second-order mass-spring-damper system, which indicates that the novel impedance control method can make the HDU equivalent to a second-order mass-spring-damper system.By the control method in this paper, the HDU can have compliance to reduce the impact caused by the severe time-variation of load force.

Appendix

ω Natural frequency of servo valve
ζ Damping ratio of servo valve
C_d Orifice flow coefficient of spool valve
C_D The desired damping
W Area gradient of spool valve
ρ Density of hydraulic oil
K_d Conversion coefficient
p_s System supply oil pressure
p_0 System return oil pressure
p_1 Inlet cavity pressure of servo cylinder
p_2 Outlet cavity pressure of servo cylinder
p_L Load pressure
$\hat{p}_L$ The observed load pressure
p_c Feedback damping pressure
C_{ip} Internal leakage coefficient of servo cylinder
C_{ep} External leakage coefficient of servo cylinder
L Total piston stroke of servo cylinder
L_0 Initial piston position of servo cylinder
A_p Effective piston area of servo cylinder
β_e Effective bulk modulus
m_t Conversion mass (including the mass of the piston, the displacement sensor, the force sensor, the connecting pipe and the oil in servo cylinder)
m_D The desired mass
x_D The desired displacement
x_p Servo cylinder piston displacement
x_p' Cylinder piston displacement without the damping control
x_v Servo valve spool displacement
x_v' Servo valve Spool displacement without the damping control
x_r Input displacement
K_{axv} Servo valve gain
K_x Displacement sensor gain
K_p Proportional gain
K Load stiffness
K_D The desired stiffness

This work is licensed under a Creative Commons Attribution 3.0 License. For more information, see http://creativecommons.org/licenses/by/3.0/.

This article has been accepted for publication in a future issue of this journal, but has not been fully edited. Content may change prior to final publication. Citation information: DOI 10.1109/ACCESS.2018.2871244, IEEE Access

K_s Closed loop system stiffness of HDU

K_s' The synthetical stiffness of HDU

B_p Viscous damping coefficient

F_L External load force

F Load force tested by force sensor (including inertia force, viscous force, elastic force and external load force, but load friction is neglected)

F' Load force tested by force sensor without the damping control

F_c Feedback damping force

F_f Friction of HDU

V_{g1} Volume of input oil pipe

V_{g2} Volume of output oil pipe

U_r Input voltage

U_p Displacement sensor feedback voltage

U_g Controller output voltage

q_1 Inlet oil flow

q_2 Outlet oil flow

Q_1 Left cavity flow of servo cylinder

Q_2 Right cavity flow of servo cylinder

β_e Effective bulk modulus

λ System pole

Reference

[1] C. Semini *et.al*."Design of HyQ -A hydraulically and electrically actuated quadruped robot. *Proc I MechE Part I: J Sys Contr Eng*, vol. 226, pp. 831-849, Aug. 2011.

[2] J. Gao *et al*., "The modeling and controlling of electrohydraulic actuator for quadruped robot based on fuzzy Proportion Integration Differentiation controller," *Proc I MechE, Part C: J Mech Eng Sci*, vol. 228, pp. 2557-2568, Sep. 2014.

[3] X.W. Rong et al., "Design and simulation for a hydraulic actuated quadruped robot," *J Mech Sci Technol*, vol. 26, no. 4, pp. 1171-1177, April 2012.

[4] M. Focchi *et al*., "Local reflex generation for obstacle negotiation in quadrupedal locomotion," International Conference on Climbing and Walking Robots and the Support Technologies for Mobile Machines, 2015, vol. 10, no. 1, pp. 443-450.

[5] Playter R.; Buehler M.; Raibert M., "BigDog," Unmanned Systems Technology VIII, Proceedings of SPIE: Bellingham, WA, USA, 2006, vol. 6230, pp. 1–6.

[6] M. Raibert *et al*., "Bigdog, the Rough-terrain Quadruped Robot," Proceedings of the 17th World Congress the International Federation of Automatic Control (IFAC), 2008, pp.1452-1458.

[7] M.T. Li *et al*., "Control of a Quadruped Robot with Bionic Springy Legs in Trotting Gait," *J Bio Eng*, vol. no. 2, pp. 188-198, Feb. 2014.

[8] K.X. Ba *et al*., "Parameters Sensitivity Analysis of Position-Based Impedance Control for Bionic Legged Robots' HDU," *Appl Sci*, vol. 7, no. 10, pp. 1035, Oct. 2017.

[9] N. Hogan, "Impedance control: An approach to manipulation: part II – implementation," *J Dyn Syst-T ASME*, vol. 107, pp. 8-16,1985.

[10] J. Maples, J. Becker, "Experiments in force control of robotic manipulators" *IEEE Robot Autom Mag*, vol. 3, pp. 695-702,1986.

[11] X. Wang *et al*., "Design of Bilateral Teleoperators for Soft Environments with Adaptive Environmental Impedance Estimation," IEEE International Conference on Robotics and Automation, Barcelona: IEEE, 2005, pp. 1127-1132.

[12] B. Heinrichs, N. Sepehri, A.B. Thornton-Trump, "Position-based impedance control of an industrial hydraulic manipulator," IEEE International Conference on Robotics and Automation, 1996, vol. 1, pp. 284-290.

[13] G. Bilodeau, E. Papadopoulos, "Model-based impedance control scheme for high-performance hydraulic joints," IEEE International Conference on Intelligent Robots and Systems, 1998, pp. 1308-1313.

[14] H. Sadjadian, H. Taghirad, "Impedance control of the hydraulic shoulder a 3-DOF parallel manipulator," IEEE International Conference on Robotics and Biomimetics, Kunming, 2006, pp. 526-531.

[15] P. Minyong *et al*., "Hybrid impedance and force control for massage system by using humanoid multi-fingered robot hand," IEEE International Conference on Systems, Man, and Cybernetics, Montreal, 2007, pp. 3021-3026.

[16] D. Ioannis, P. Evangelos, "Impedance model-based control for an electrohydraulic Stewart platform," *Eur J Control*, vol. 15, pp. 560-577, 2009.

[17] A. Irawan, K. Nonami, "Optimal impedance control based on body inertia for a hydraulically driven hexapod robot walking on uneven and extremely soft terrain," *J Field Robot*, vol. 28, pp. 690-713, 2011.

[18] S. Lee , J. Cho, S. Park, "Position-based impedance control of a hydraulic actuator for a walking robot," Adaptive Mobile Robotics-Proceedings of the 15th International Conference on Climbing and Walking Robots and the Support Technologies for Mobile Machines(CLAWAR), Baltimore, 2012, pp. 781-788.

[19] B. Ugurlu *et al*., "Dynamic trot-walking with the hydraulic quadruped robot- HyQ: Analytical trajectory generation and active compliance control," IEEE International Conference on Intelligent Robots and Systems, New Horizon, 2013, pp. 6044-6051.

[20] M. Sharifi, S. Behzadipour, G. Vossoughi, "Nonlinear model reference adaptive impedance control for human-robot interactions," *Control Eng Pract*, vol. 32, pp. 9-27, 2014.

[21] A. Irawan *et al*., "Adaptive impedance control with compliant body balance for hydraulic-actuated hexapod robot," 10th International Conference on Motion and Vibration Control, Tokyo, 2010, pp. 1-9.

[22] Q. Xu, "Robust Impedance Control of a Compliant Microgripper for High-Speed Position/Force Regulation," *IEEE T Ind Electron*, vol. 62, no. 2, pp. 1201-1209, Feb. 2015.

[23] Ba K.X., Yu B., Gao Z.J., et al., "Parameters Sensitivity Analysis of Position-Based Impedance Control for Bionic Legged Robots' HDU," Appl Sci, vol. 7, no. 10, pp. 1035, Oct. 2017.

[24] Ba K.X., Yu B., Kong X.D., et al., "The dynamic compliance and its compensation control research of the highly integrated valve-controlled cylinder position control system," Int J Control Autom, vol. 15, no. 4, pp. 1814-1825, April 2017.

[25] X.D. Kong *et al*., "Research on the force control compensation method with variable load stiffness and damping of the hydraulic drive unit force control system". *Chin J Mech Eng*, vol. 29, no. 3, pp. 454-464, March 2016.

This work is licensed under a Creative Commons Attribution 3.0 License. For more information, see http://creativecommons.org/licenses/by/3.0/.